Neuroscience Letters 528 (2012) 137–142

Contents lists available at SciVerse ScienceDirect

Neuroscience Letters

journal homepage: www.elsevier.com/locate/neulet

Adaptive estimation of EEG for subject-specific reactive band identification and improved ERD detection

Yubo Wang[a], Kalyana C. Veluvolu[a,*], Jin-Ho Cho[a], M. Defoort[b]

[a] College of IT Engineering, Kyungpook National University, Daegu 702-701, South Korea
[b] LAMIH, CNRS FRE 3304, Univ. Lille Nord de France, UVHC, F-59313, Valenciennes, France

HIGHLIGHTS

- Model EEG mu-rhythm with BMFLC for time–frequency decomposition.
- Subject-specific reactive band for ERD is identified.
- Study is conducted for reactive band identification and improved ERD detection.
- Selection of reactive band improves the ERD detection by 22% and classification accuracy by 10%.

ARTICLE INFO

Article history:
Received 17 May 2012
Received in revised form 18 August 2012
Accepted 1 September 2012

Keywords:
BMFLC
EEG
Subject reactive band
ERD detection
Adaptive filtering
BCI

ABSTRACT

The event-related desynchronization (ERD) is a magnitude decrease phenomenon which can be found in electroencephalogram (EEG) mu-rhythm in a certain narrow frequency band (reactive band) during different sensorimotor tasks and stimuli. The success of ERD detection depends on proper identification of subject specific reactive band. An adaptive algorithm band limited multiple Fourier linear combiner (BMFLC) is employed in this paper for identification of subject specific reactive band for real-time ERD detection. With the time–frequency mapping obtained with BMFLC, a procedure is formulated for reactive band identification. Improved classification is obtained by applying this method to a standard BCI data set compared to traditional ERD detection methods. Study conducted with 8 subjects drawn from BCI Competition IV data set show a 22% increase in ERD and 10% improvement in classification with the proposed method compared to standard ERD based classification.

1. Introduction

Event-related desynchronization (ERD) is a magnitude decrease phenomenon in a certain frequency band which can be found in EEG, ECoG and MEG during sensory and cognitive processing and motor behavior. Since a hand movement μ-rhythm (6–14 Hz) ERD can be found in most subjects, the sensorimotor ERD pattern has received significant attention in neuroscience research [10,15]. It was shown that 93% of subjects successfully controlled an ERD based BCI device with over 60% accuracy. With this robustness, the sensorimotor ERD can be considered as an efficient control signal for BCI applications [6].

The sensorimotor ERD occurs in the μ-rhythm (6–14 Hz). In most subjects the ERD can only be seen in a specific narrow band [15]. Two classical methods short-time power spectra and wavelets transform are widely adopted for subject's reactive band determination [15]. In the short-time power spectra comparison, two power spectra for reference and activity periods are computed for all event-related trials with short-time Fourier transform (STFT). By comparing the difference between the two power spectra, the region with significant difference was computed as the most reactive band. The drawback of this method lies with the low frequency resolution. The wavelet transform solves the problem of frequency resolution; however its need for high computation remains a major drawback for real-time applications. Also wavelet transform suffers from tradeoff between temporal and spectral resolution similar to STFT [1]. In [5], the EEG signal is band-pass filtered in the frequency range of 7–34 Hz and ERD/ERS is computed with classical method [15] using fixed narrow frequency bands. This method suffers from low frequency resolution.

To overcome the problems, such as limited frequency resolution, non-causality and high computation requirement, in this paper a recently developed method BMFLC is employed [17]. The BMFLC relies on least mean squares (LMS)-based adaptive filter that estimates all individual frequency components in a pre-defined band of interest. A statistical parameter is employed for automatic identification of subject-specific reactive band. With the study conducted on 8 subjects, an improved ERD detection and better classification

* Corresponding author. Tel.: +82 53 950 7232; fax: +82 53 950 5505.
E-mail address: veluvolu@ee.knu.ac.kr (K.C. Veluvolu).

0304-3940/$ – see front matter © 2012 Elsevier Ireland Ltd. All rights reserved.
http://dx.doi.org/10.1016/j.neulet.2012.09.001

accuracy are obtained with the proposed method in comparison with traditional ERD detection methods.

2. Methods

Since, EEG is comprised of quasi-periodic or quasi-sinusoidal signals characterized by coupled harmonically related frequencies, there have been several Fourier based works [17]. A method that tracks energy distribution of every frequency component within a pre-defined frequency band is desirable for accurate ERD detection and subject specific reactive-band selection. In this section, time–frequency analysis of EEG in the range of 6–14 Hz is performed by modeling EEG with BMFLC [17].

2.1. Time–frequency modeling of EEG with BMFLC

To model the unknown μ-rhythm, we consider the signal to be distributed in the band of $[\omega_1 - \omega_n]$ and then divide the frequency band of interest into 'n' finite number of divisions $\Delta\omega$ [17] to form BMFLC:

$$y_k = \sum_{r=1}^{n} a_{rk} \sin(\omega_r k) + b_{rk} \cos(\omega_r k) \tag{1}$$

where y_k denotes the modeled EEG signal at sampling instant k. a_{rk}, b_{rk} represents the adaptive weights corresponding to the frequency ω_r at time instant k. BMFLC adopts the LMS algorithm to adapt the weights a_{rk}, b_{rk} in (1) to the incoming unknown signal. The algorithm can be stated as follows:

$$\mathbf{x}_k = \left\{ \begin{array}{l} [\,\sin(\omega_1 K) \quad \sin(\omega_2 K) \quad \cdots \quad \sin(\omega_n K)\,]^T \\ [\,\cos(\omega_1 K) \quad \cos(\omega_2 K) \quad \cdots \quad \cos(\omega_n K)\,]^T \end{array} \right\}$$

$$y_k = \mathbf{w}_k^T \mathbf{x}_k \tag{2}$$

$$\varepsilon_k = s_k - y_k \tag{3}$$

$$\mathbf{w}_k = \mathbf{w}_k + 2\eta \mathbf{x}_k \varepsilon_k \tag{4}$$

where $\mathbf{w}_k = \left[\, a_{1k} \quad \cdots \quad a_{nk}, \quad b_{1k} \quad \cdots \quad b_{nk} \,\right]^T$ and $\mathbf{x}_k$ are the adaptive weight vector and reference input vector respectively. s_k is the reference signal, ε_k represents the error term and η is an adaptive gain parameter. Input signal amplitude and phase are estimated by the adaptive vector $\mathbf{w}_k$. For more details, see [17,18]. The accuracy of modeling depends on the frequency spacing $\Delta\omega/2\pi$. A value of 0.1–0.5 Hz for $\Delta\omega/2\pi$ is optimum for estimation of band limited signal to obtain an accuracy of 96–98% [17,18].

Based on (1) and (2), the weight vectors in $\mathbf{w}_k$ represents the Fourier coefficients of the modeled EEG signal at time instant k. In order to evaluate the individual frequency components at any given time instant k, we compute the square-root of the sum of squares of the sine and cosine components to obtain

$$\mathbf{w}_k^f = \left[\frac{\sqrt{a_{1k}^2 + b_{1k}^2}}{2} \quad \cdots \quad \frac{\sqrt{a_{nk}^2 + b_{nk}^2}}{2} \right]^T \tag{5}$$

where $\mathbf{w}_k^f$ is the absolute weight vector of the frequency components at instant k. The time–frequency weight matrix termed D can be obtained for the signal with m samples as

$$D = \left[\, \mathbf{w}_1^f \quad \cdots \quad \mathbf{w}_k^f \quad \cdots \quad \mathbf{w}_m^f \,\right] \tag{6}$$

This time–frequency decomposition contains the absolute values of all the frequency components with frequency spacing/resolution $\Delta\omega$ and time resolution k. As $D(k,f)$ represents the amplitude of frequency component at time instant k, the power for all the frequency components can be computed as

$$P(k,f) = D(k,f) \times D(k,f) \tag{7}$$

where $P(k,f)$ represents the power of frequency component f at time instant k. Hence the P matrix represents the power distribution of the band limited signal, the average of the row vector of each frequency component over time interval provides the average power of the corresponding frequency component in the given μ-rhythm.

2.2. Reactive band Identification

In [15] it was shown that selection of most reactive-frequency bands for subjects when compared with standard frequency bands has higher ERD detection success rate. The difference in the mean of the weights between rest and activity will provide the qualitative measure of each frequency component variation between the rest and imagery/real movements of the subject. The average power during the rest (P_{Rest}) and movement imagery (P_{Imag}) can be obtained as

$$P_{\text{Rest}}(f) = \frac{\sum_{k=k_1}^{k_2} P(k,f)}{k_2 - k_1}; \qquad P_{\text{Imag}}(f) = \frac{\sum_{k=k_3}^{k_4} P(k,f)}{k_4 - k_3},$$

$$P_{\text{Diff}} = P_{\text{Rest}} - P_{\text{Imag}}$$

where, $k = [k_1 \quad k_2]$ is the time period during rest and $k = [k_3 \quad k_4]$ is the time period during imagery/real movement. The band of frequencies that correspond to the largest difference in average power (P_{Diff}) can be identified as the subject's reactive band. Although, the region with the high difference can be identified, selection of reactive band and bandwidth remains as a problem. To overcome this issue, this paper uses a statistical parameter developed in [18] as a norm to identify the reactive band. We define the power ratio % as

$$\Delta = \frac{A_{\text{opt}}}{A_\mu} \times 100$$

where A_{opt} is the area under the P_{Diff} curve for the selected reactive band and A_μ is the total positive area under the P_{Diff} curve for the μ-band. The band that provides the maximum area under the P_{Diff} curve for the given bandwidth is chosen as A_{opt}. Since A_{opt}, A_μ represent the average power in the optimal band and μ-band, Δ represents % average energy ratio of selected reactive band to the μ-band. A statistical analysis of this parameter will reveal the band characteristics, and a proper selection of this parameter will lead to automatic identification of the reactive band.

2.3. ERD estimation

As precise time–frequency power distribution is available in the form of P matrix, ERD can be directly calculated. To compute the spectrum band-power in a specific frequency band, we compute the sum of individual power components at a given instant k as:

$$P_R(k) = \sum_{f=f_1}^{f_2} P(k,f) \tag{8}$$

where (f_1, f_2) is the identified reactive band of the subject. An ERD estimate [15,5] is obtained by computing the relative band-power with respect to reference time-window. If we denote $P_{\text{ref}} = \sum_{k=k_1}^{k_2} P_R(k)/(k_2 - k_1)$ as the averaged reference power during the reference period, then ERD(k) can be estimated as:

$$\text{ERD}(k) = \frac{P_R(k) - P_{\text{ref}}}{P_{\text{ref}}} \tag{9}$$

Table 1
Subjects with optimal band power ratio.

Bandwidth	No. of events with Δ %			
	20–50	50–70	70–85	85–100
BW^{+} = 2 Hz	6	4	5	1
BW^{+} = 2.4 Hz	6	3	4	3
BW^{+} = 3 Hz	2	6	3	5
BW^{+} = 3.6 Hz	1	3	5	7

2.4. Data for analysis

For analysis, 8 subjects EEG data drawn from BCI Competition IV [3] data set 2a is used in this paper. Four classes of cue-based motor imagery tasks were carried out, namely the imagination of movement of the left hand, right hand, both feet and tongue. For more details, see [3]. For hand movement imagery, EEG data from the electrodes C3 and C4, placed over the sensorimotor cortex according to 10/20 international system, where the μ-rhythm originates, is selected for analysis. In order to enhance the signal-to-noise ratio of the EEG data, as suggested in [13], a small Laplacian spatial filter is applied to obtain the EEG signal at C3 and C4 locations.

3. Results

For modeling the μ-rhythm, the data is band-pass filtered between 6 and 14 Hz. We choose the following parameters for the BMFLC: $f_1 = 6$ Hz, $\omega_1 = 2\pi f_1$, $f_n = 14$ Hz, $\omega_n = 2\pi f_n$ with frequency spacing $\Delta\omega/2\pi = 0.2$ Hz and adaptive gain $\eta = 0.015$. BMFLC was used to model the EEG μ-rhythm for each trial separately with a 1 s moving window and 0.5 s overlap. The first 0.5 s was discarded as the weights does not adapt completely. BMFLC is applied to all trials (right hand C3 (RH) imagery, left hand C4 (LH) imagery) separately. The accuracy of EEG modeling with BMFLC is quantified with % accuracy that is defined as:

$$\%\,\text{Accuracy} = \frac{\text{RMS}(s) - \text{RMS}(\varepsilon)}{\text{RMS}(s)} \times 100 \tag{10}$$

where $\text{RMS}(s) = \sqrt{\left(\sum_{k=1}^{m} s_k\right)/m}$. The mean and standard deviation (±STD) of % accuracy with BMFLC for 8 subjects for all trials is obtained as 98.64 ± 0.24. As BMFLC is applied to all trials separately, the obtained time–frequency weight matrices (D in (6)) for all trials is averaged to obtain the subject time–frequency map for a specific motor imagery task. For illustration, the averaged time–frequency maps for three subjects are shown in Fig. 1(a1)–(c1).

From the cue sequence (cue presents at $t = 2$ s), the reference periods for the rest and motor imagery task are set to be $t = 0.5$–1.5 s and $t = 3$–4.5 s respectively. With the methodology presented in Sections 2.1 and 2.2, the power difference between the rest and active part for all frequencies in the μ-band is computed for all trials and the average plots are shown in Fig. 1(a2)–(c2) for three subjects. To analyze the effect of bandwidth BW^{+}, the power ratio (Δ) for varying bandwidths (2 Hz, 2.4 Hz, 3 Hz and 3.6 Hz) is computed for all subjects (C3 (RH) and C4 (LH) events). The number of events (C3 (RH) and C4 (LH) events) for various bandwidth BW^{+} and Δ selection are tabulated in Table 1. The distribution of the events in the table reveals that an average Δ of 40–65% exists in most subjects. The power ratio Δ provides a measure of how good is the selected reactive band. For only few events, an increase in BW^{+} increased the energy or power ratio. Hence in this study, $\Delta \geq 50$ can be chosen as the basis to identify the subject-specific reactive bandwidth. For subjects with low $\Delta < 30$, bigger $BW^{+} > 2$ can be selected to adjust the Δ. However for ease of classifier implementation, a reactive bandwidth of 2 Hz is selected for all the subjects in this paper. For a reactive band with $BW^{+} = 2$, Δ for all subjects and events are tabulated in Table 2. Most of the subjects have $\Delta > 50$. The average time–frequency decomposition maps and the identified reactive bands for three subjects are presented in Fig. 1(a1)–(c1). The identified reactive bands of the subjects are co-related with their time–frequency maps as shown in Fig. 1(a2)–(c2). For subject #1 C3 (RH) event, energy decrease can be seen within 0.5 s before or after the cue onset as shown in Fig. 1(a1). This energy decrease can be related to the ERD phenomenon during the movement imagery task. The power ratio (Δ) is obtained as 43.2 for $BW^{+} = 2$ Hz. The power difference curve clearly shows the existence of the reactive band in Fig. 1(a2). The reactive band identified for all subjects are shown in Table 2. The results of reactive band selection for the three subjects are shown in Fig. 1(a2)–(c2). Among the three subjects, ERD can be identified in different frequency bands. For subject #3 C4 (LH) event, the identified reactive band is shown in Fig. 1(b2) with $\Delta = 32.5$. However for subject #7 C3 (RH) event, the condition $\Delta \geq 50$ is satisfied and the identified reactive band (9–11 Hz) is shown in Fig. 1(c2). For most of the subjects, both the electrode positions (C3 and C4) exhibit similar reactive band characteristics. ERD phenomenon for three subjects with the reactive band and complete μ-band are shown in Fig. 1(a3)–(c3). The difference of the maximum ERD and the minimum ERD value within the reference period is chosen for comparison of the proposed reactive band ERD% and the μ-band ERD% in Table 2.

In order to test the variation of the estimated average over all trials, bootstrap method (with 500 times re-sampling) [5] is employed for estimating the 95% confidential interval (CI) for time and frequency. The estimated 95% CI is then transformed to the form of ERD with (9). The results of 3 subjects with the estimated 95% CI are shown in Fig. 1(a4)–(c4) for μ-band and in Fig. 1(a5)–(c5) for reactive band respectively. ERD value for a sample may be considered significant with 95% confidence interval when both upper and lower confidence values of this sample show the same sign. With the proposed method for ERD estimation, it is clear that the ERD values always lie within the 95% CI.

Since, the goal is to apply the proposed method for BCI applications, ERD based classifier [12] is used to classify different limb movements (RH, LH) with the proposed method. As the classifier relies on the power changes in the specified frequency band, the power of the signal in the identified subject-specific reactive band obtained with BMFLC can be readily used for classification. The signal power in the 2 Hz reactive-band is considered as the feature vector. With 0.2 Hz frequency spacing, the feature space dimension will be 2 channels × 10 frequency weights (2/0.2) for each sample. Similar to [16], the classification is made in the 1 s window after the cue onset. By selecting 3–4 s as the decision window, a decision is made at every 240 ms in the 1 s window (four decisions in the 1 s window). The data of BMFLC was averaged in the decision interval to get the power estimate. Every element in the feature vector is an averaged power value in (7) and is given by

$$p_i^f = \frac{1}{N} \sum_{t=i-N}^{i} P(t, f) \tag{11}$$

where i is the time index of a particular decision point, f is frequency index and N is the number of samples in that time interval. Thus, the feature vector is designed as

$$\mathbf{F}_{\text{BMFLC}}^{i} = \left(p_{i,(C3)}^{f_{\min}} \quad \cdots \quad p_{i,(C3)}^{f_{\max}}, \quad p_{i,(C4)}^{f_{\min}} \quad \cdots \quad p_{i,(C4)}^{f_{\max}} \right)^{T} \tag{12}$$

where $f_{\min}$ and $f_{\max}$ are the lower and upper bound of the identified reactive band, C3 and C4 are the channel indices. The linear discriminate analysis (LDA) is considered as a robust classifier for classifying the EEG power changes [8]. And its generalization, quadratic discriminate analysis (QDA) [2] is shown to have superior performance when the wavelets coefficients are used as features for

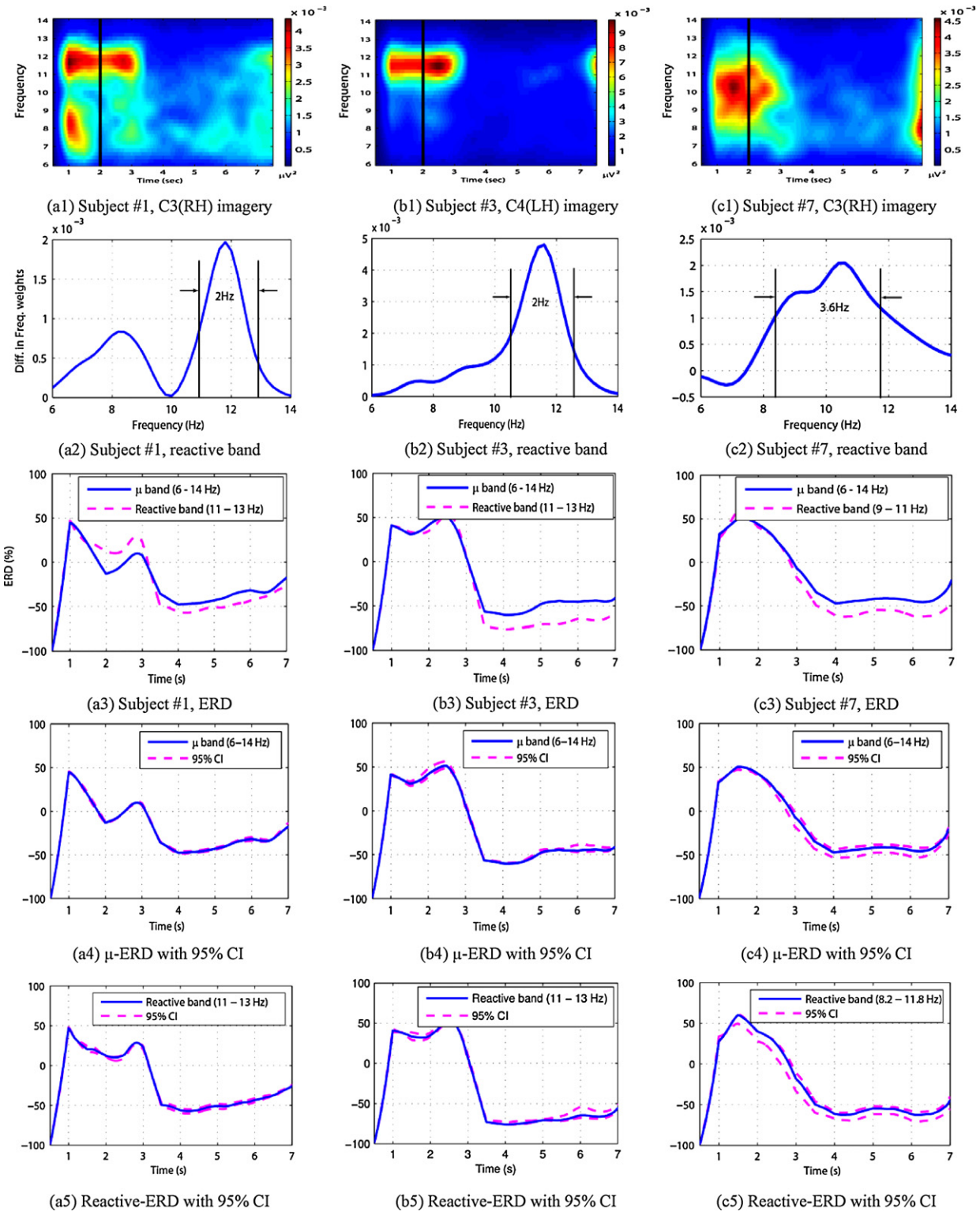

Fig. 1. (a1, b1, c1) Time frequency decomposition of power with the proposed method for three subjects (S#1, S#3 and S#7, the dark line indicates onset of the stimulus); (a2–c2) Reactive band identification for three subjects; (a3–c3) Comparison of ERD % in μ-band and the identified reactive band; (a4–c4) 95% CI for ERD in μ-band; (a4–c4) 95% CI for ERD in identified reactive band.

classification [7]. Since BMFLC provides power of frequency components in EEG, both LDA and QDA are used for classification [7] in this paper. For comparison, band power based classifier is also implemented. The signal is first band pass filtered into 3 Hz frequency bins (7–10, 9–12, 11–14) with 1 Hz overlap [14]. Similar to the earlier method, every 240 ms data are averaged to form one feature vector with dimension 2 channels × 3 power samples. The obtained feature vectors are fed to both LDA and QDA.

Similar to [16], we assume that the classifier produces decisions at a constant rate, i.e. every 240 ms. In The BCI system can be more interactive by providing feedback on the user performance for constant improvement. The classifier is trained at four points [16]. In

Table 2
Comparison of ERD (%) in μ-band and reactive band.

2 Sessions × 6 runs × 48 trails		Δ (reactive band)	Identified reactive band (Hz)	max{ERD%}–min{ERD%}		
				μ-Band	Reactive band	Improvement
S#1	C4(LH)	32.2	7–9	88.7	100.4	11.7
	C3(RH)	43.2	10–12	92.2	95.7	3.5
S#2	C4(LH)		No band(7–14)			
	C3(RH)		No band(7–14)			
S#3	C4(LH)	32.5	11–13	111.1	130.9	19.8
	C3(RH)	26.8	11–13	131.7	150.8	19.1
S#4	C4(LH)	36.9	10–12	44.9	91.9	47.0
	C3(RH)	76.6	10.4–12.4	71.4	116.1	44.7
S#5	C4(LH)		No band(7–14)			
	C3(RH)	63.9	9–11	35.0	47.6	12.6
S#6	C4(LH)	78.8	11–13	97.5	113.1	15.7
	C3(RH)	59.7	11–13	40.5	69.2	28.7
S#7	C4(LH)	51.6	9–11	97.9	121.6	23.7
	C3(RH)	54.4	9–11	113.3	137.6	24.3
S#8	C4(LH)	85.1	9–11	89.8	114.5	24.7
	C3(RH)	74.1	9–11	69.8	100.9	31.1
S#9	C4(LH)	83.6	9.8–11.8	144.1	152.3	8.2
	C3(RH)	70.5	10.2–12.2	108.2	116.1	7.9

order to make 4 decisions, 4 LDA or QDA classifiers are trained with the data of that specific decision point for all the trials. For each decision point, 10×10-fold cross validations [16] are used. The accuracy obtained from $k \times k$ fold cross validation [16] is a robust measure of the performance of the classifier. In this technique, the data is divided into 10 parts randomly, where 9 sections are used for training and 1 section is used for testing. The accuracy of the classifier is based on the test data and the overall accuracy at each decision point is averaged over 100 times for validation.

The box plots of the classification accuracy for all subjects at all decision points are shown in Fig. 2. It is clear that BMFLC based LDA and QDA has higher median classification accuracy compared to its respective band-power counterparts. An independent t-test has been applied to test whether the results are significantly different.

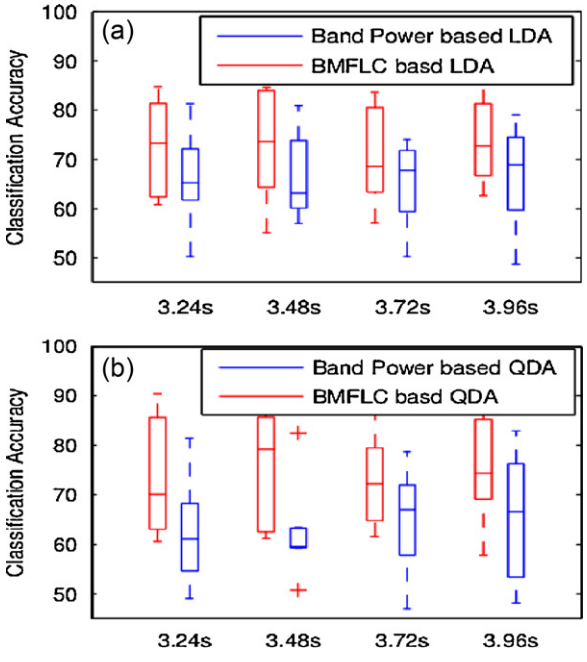

Fig. 2. Average classification accuracy at four decision points for all subjects.

For the BMFLC based LDA classifier the classification accuracy has higher interquartile range and the results are also left-skewed compared to band power based LDA as shown in Fig. 2(a). However, the average accuracy of BMFLC based LDA is superior compared to band power based LDA ($t = 11.770$, $\alpha = 0.001$).

BMFLC based QDA also performed better compared to band power based QDA as shown in Fig. 2(b). Although the BMFLC based QDA has slightly higher interquartile range compared to band power based QDA, the median of accuracy of band power based QDA is lower than the lower quartile of BMFLC based QDA. Further the average accuracy obtained with BMFLC based QDA for all decision points was 74.7% compared to 63.97% obtained with band power based QDA. An independent t-test show that this difference in accuracy is significant ($t = 10.975$, $\alpha = 0.001$). This clearly highlights that a classification boundary associated with QDA is more appropriate to pair with BMFLC to achieve high accuracy.

4. Discussions and conclusions

With the proposed method an average of 22% improvement is obtained in ERD detection for hand motor imagery tasks over all subjects. Of all the subjects, reactive band cannot be identified for subject #2 (C3 and C4) and subject #5 (C3). The band is distributed and so the complete μ-band is considered as the reactive band. The power ratio Δ provides a measure of how good is the selected reactive band. For subjects with distinctive reactive band (e.g. Subject #1, Fig. 1(a2)), a high value for Δ can be chosen for further improvement. For some subjects (subject #1 and #4), the reactive band lies slightly outside the μ-band (7–14 Hz). The time–frequency map in Fig. 1(a1) clearly shows the occurrence of ERD in the frequency range of 6–9 Hz. Hence it is advisable to analyze the reactive band characteristics in the range of 6–14 Hz for identification. The proposed method is simple and is more suitable for ERD based real-time BCI applications. Both the classifiers LDA and QDA showed improved classification for motor imagery tasks.

Recently, a generalized ERD estimation method [11] that incorporates pre-stimulus activity is developed. The method requires a specific experiment protocol to identify the dynamic reference in the EEG signal. As BMFLC is a fixed frequency amplitude tracking algorithm, it can be directly applied to the dynamic reference

EEG data for generalized ERD estimation. Earlier methods relied on average procedure or selection of fixed bands for reactive band identification [15]. For ERD detection with matching pursuit algorithm [4], the computation requirement is high and is not suitable for real-time implementation. In [9], the time–frequency analysis of EEG signal is obtained with local discriminant bases where only 4 Hz frequency resolution is obtained. All the above discussed methods [4,9] decompose the signal into wide frequency bands whereas BMFLC relies on a narrow band and hence good classification can be obtained. Although, the application of BMFLC is limited to analysis of μ-band ERD in this paper, the method is applicable to other frequency bands in EEG. ERD and ERS can be estimated simultaneously by employing two BMFLC algorithms separately in their frequency range of interest.

Acknowledgement

This research was supported by Kyungpook National University Research Fund, 2011.

References

[1] D.P. Allen, C.D. MacKinnon, Time frequency analysis of movement-related spectral power in EEG during repetitive movements: a comparison of methods, Journal of Neuroscience Methods 186 (2010) 107–115.
[2] S. Bhattacharyya, A. Khasnobish, S. Chatterjee, A. Konar, D.N. Tibarewala, Performance analysis of LDA, QDA and KNN algorithms in left–right limb movement classification from EEG data, in: Proceedings of 2010 International Conference on Systems in Medicine and Biology, Kharagpur, India, 2010.
[3] C. Brunner, M. Naeem, R. Leeb, B. Graimann, G. Pfurtscheller, Spatial filtering and selection of optimized components in four class motor imagery data using independent components analysis, Pattern Recognition Letters 28 (2007) 957–964.
[4] M.J. Durka, D. Ircha, D. Neuper, G. Pfurtscheller, Time–frequency microstructure of event-related electro-encephalogram desynchronisation and synchronisation, Medical Biological Engineering Computing 39 (2001) 315–321.
[5] B. Graimanna, J.E. Huggins, S.P.a.P.G. Levineb, Visualization of significant ERD/ERS patterns in multichannel EEG and ECoG data, Clinical Neurophysiology 113 (2002) 43–47.
[6] C. Guger, G. Edlinger, W. Harkam, I. Niedermayer, G. Pfurtscheller, How many people are able to operate an EEG-based brain–computer interface (BCI)? IEEE Transactions on Neural Systems and Rehabilitation Engineering 11 (2003) 145–147.
[7] T. Hastie, R. Tibshirani, J. Friedman, Linear methods for classification, in: The Elements of Statistical Learning, Springer, New York, USA, 2001, p. 101 (Chapter 4).
[8] P. Herman, G. Prasad, T.M. McGinnity, D. Coyle, Comparative analysis of spectral approaches to feature extraction for EEG-based motor imagery classification, IEEE Transactions on Neural Systems and Rehabilitation Engineering 16 (2008) 317–326.
[9] N.F. Ince, S. Arica, A. Tewfik, Classification of single trial motor imagery EEG recordings with subject adapted non-dyadic arbitrary time–frequency tilings, Journal of Neural Engineering 3 (2006) 235–244.
[10] Y. Ku, B. Hong, X. Gao, S. Gao, Spectra-temporal patterns underlying mental addition: an ERP and ERD/ERS study, Neuroscience Letters 472 (2010) 5–10.
[11] S. Lemm, K.R. Muller, G. Curio, A generalized framework for quantifying the dynamics of EEG event-related desynchronization, PLoS Computational Biology 5 (8) (2009) e1000453.
[12] F. Lotte, M. Congedo, A. Lecuyer, F. Lamarche, B. Arnaldi, A review of classification algorithm for EEG-based brain–computer interface, Journal of Neural Engineering 4 (2007) R1–R13.
[13] D.J. McFarland, L.M. McCane, S.V. David, D.J. Wolpaw, Spatial filter selection for EEG-based communication, Electroencephalography and Clinical Neurophysiology 103 (1997) 386–394.
[14] D.J. McFarland, J.R. Wolpaw, Sensorimotor rhythm-based brain computer interface (BCI): model order selection for autoregressive spectral analysis, Journal of Neural Engineering 5 (2008) 155–162.
[15] G. Pfurtscheller, F.H. Lopes da Silva, Event-related EEG/MEG synchronization and desynchronization: basic principles, Clinical Neurophysiology 110 (1999) 1842–1857.
[16] G. Pfurtscheller, C. Neuper, A. Schlogl, K. Lugger, Separability of EEG signals recorded during right and left motor imagery using adaptive autoregressive parameters, IEEE Transactions on Neural Systems and Rehabilitation Engineering 6 (1998) 316–325.
[17] K.C. Veluvolu, W.T. Ang, Estimation and filtering of physiological tremor for real-time compensation in surgical robotics applications, International Journal of Medical Robotics and Computer Assisted Surgery 6 (2010) 334–342.
[18] K.C. Veluvolu, Y. Wang, S.S. Kavuri, Adaptive estimation of EEG-rhythms for optimal band identification in BCI, Journal of Neuroscience Methods 203 (2012) 163–172.